

© Copyright 2007 American Meteorological Society (AMS). For permission to reuse any portion of this work, please contact permissions@ametsoc.org. Any use of material in this work that is determined to be “fair use” under Section 107 of the U.S. Copyright Act (17 U.S. Code §107) or that satisfies the conditions specified in Section 108 of the U.S. Copyright Act (17 USC § 108) does not require the AMS’s permission. Republication, systematic reproduction, posting in electronic form, such as on a website or in a searchable database, or other uses of this material, except as exempted by the above statement, requires written permission or a license from the AMS. All AMS journals and monograph publications are registered with the Copyright Clearance Center (<https://www.copyright.com>). Additional details are provided in the AMS Copyright Policy statement, available on the AMS website (<https://www.ametsoc.org/PUBSCopyrightPolicy>).

Access to this work was provided by the University of Maryland, Baltimore County (UMBC) ScholarWorks@UMBC digital repository on the Maryland Shared Open Access (MD-SOAR) platform.

Please provide feedback

Please support the ScholarWorks@UMBC repository by emailing scholarworks-group@umbc.edu and telling us what having access to this work means to you and why it’s important to you. Thank you.

Geoelectric Monitoring of Wind-Driven Barotropic Transports in the Baltic Sea

JENNY A. U. NILSSON

Department of Meteorology/Physical Oceanography, Stockholm University, Stockholm, Sweden

PETER SIGRAY

Department of Meteorology/Physical Oceanography, Stockholm University, and Applied Marine Research, Swedish Defense Research Agency (FOI), Stockholm, Sweden

ROBERT H. TYLER

Applied Physics Laboratory, University of Washington, Seattle, Washington

(Manuscript received 1 November 2005, in final form 29 August 2006)

ABSTRACT

The possibility of using data from a cable-based observational system for long-term monitoring of barotropic flow in the Baltic Sea was investigated. Measurements were made of the induced potential differences between Visby on the island of Gotland and Västervik on the Swedish mainland and a yearlong period was studied in order to ensure the presence of seasonal fluctuations. The predictions from a 2D electric-potential model, forced by velocity fields from a shallow-water circulation model, proved to be well correlated with the observations. A winter and a summer period were selected for a thorough analysis, the results of which indicated a stronger correlation during winter. This implies that the relative importance of the barotropic forcing tends to weaken during summer. The spatial coverage of the induced potential differences for the cable region was found to encompass a considerable part of the Baltic proper. The correlation study indicated that the winter circulation in the Baltic proper showed “broad-scale” motion, whereas summer conditions were characterized by a barotropic gyre. An overall result of the investigation is that geoelectric monitoring is capable of providing useful data for oceanographic purposes.

1. Introduction

The Baltic Sea (cf. Fig. 1) is one of the largest semienclosed seas in the world. Its hydrography has been monitored since the early 1900s, and the nature of the circulation has been the subject of intense research for decades. The basin has a large drainage area, and the resulting freshwater flux gives rise to a pronounced stratification. The brackish surface layer discharge from the Baltic Sea to the Danish Sounds is associated with a deep-water inflow. This high-saline bottomwater inflow forms a dense pool in the Arkona Basin, whereafter it cascades from basin to basin until it finally reaches the Western Gotland Deep. As a result of these

overflows a permanent halocline is formed at a depth of 60–70 m in the Baltic proper.

The complex circulation of the Baltic Sea is influenced by several meteorological factors. The predominant forcing is exerted by wind, air pressure differences, inflow, river discharge, precipitation, and evaporation, the relative importance varying from location to location. For the Baltic proper, wind forcing on time scales of days gives rise to barotropic flows, whereas for the forcing of longer periods, the importance of baroclinicity increases (cf. Pizarro and Shaffer 1998).

One of the main problems when analyzing the dynamics of the Baltic Sea circulation is the lack of continuous field measurements. This dearth of observations was pointed out by Lehmann et al. (2002), who underlined that no comprehensive observations of currents and upwelling in the Baltic Sea are available. One explanation for the sparseness of data is that this shallow sea is a vulnerable environment for conventional oceanographic instrumentation because of the intense

Corresponding author address: Jenny A. U. Nilsson, Department of Meteorology/Physical Oceanography, Stockholm University, SE-106 91 Stockholm, Sweden.
E-mail: jennyn@misu.su.se

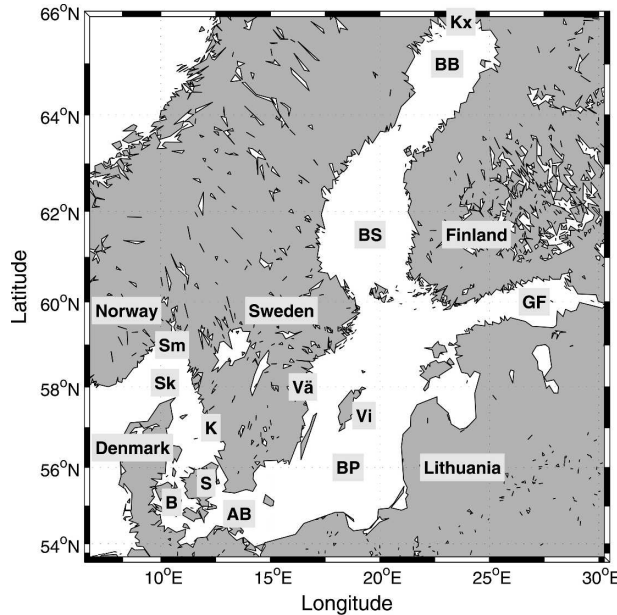


FIG. 1. Map of the Baltic Sea area, showing geographic sites: the Danish Belts (B), the Sound (S), the Kattegat (K), the Skagerrak (Sk), Smögen (Sm), the Arkona Basin (AB), the Baltic proper (BP), Västervik (Vă), Visby on the island of Gotland (Vi), the Gulf of Finland (GF), the Bothnian Sea (BS), the Bay of Bothnia (BB), and Kalix (Kx).

fishery. To overcome these problems durable sensors have to be employed, where a useful methodology is based on measuring induced “voltages” (i.e., electric potential differences). The viability of applying this technique was first demonstrated by Faraday in 1832. However, the first successful long-term observations were started by Sanford (1982) on the basis of a retired telephone cable. This conductor was later damaged and an in-service undersea telephone cable was instead taken into use (Larsen 1992). The advantage of using telecommunication cables is that they are generally buried in the seafloor, hereby having the degree of robustness required for long-term observations. An additional benefit is that the cable operators repair damages swiftly.

Before an analysis of the estimated transports can be undertaken, potential differences have to be converted into flow variables. An attempt to solve this problem was presented already by Longuet-Higgins et al. (1954), who introduced the concept of the k factor, which takes into account the effect of conductivity variations in the sea and in the sediments. Although this compensation assumes that the process being investigated manifests channel flow characteristics, the advantage of the method is its simplicity. It can, however, seldom be used for accurately determining the influence of conductivity variations in areas with even moderately complex to-

pography. An alternative procedure was presented by Spain and Sanford (1987), based on an experiment where the potential difference attenuation caused by conductivity variations was investigated by combining data from two different velocity profilers.

Sigray et al. (2004) implemented an observational system based on a fiber-optic telecommunication cable between Västervik on the Swedish mainland and Visby on the island of Gotland. This cable is located such that it is possible to monitor the bulk flow of the Baltic proper. The investigation was restricted to December 1999, which was an exceptionally stormy month, and made use of the k -factor method to convert potential differences to flow estimates before comparing the observed flow with estimates based on sea level data from two tidal gauges.

In the present study a different approach will be used. It is demonstrated that for a range of frequencies the Visby–Västervik cable data accurately represent ocean transport across the section and therefore are capable of providing a robust integral constraint for models of Baltic flow variability. This is shown by comparing the observational data to the potential differences from a two-dimensional (2D) electric-potential model, which in turn is based on a shallow-water circulation model. For these purposes only, frequencies in the range from 30 h to 2 weeks will be considered, as the primary interest is on barotropic processes in the Baltic Sea. Although it is likely that the Visby–Västervik data also describe ocean variability outside this frequency band, this cannot be validated using the method to be described here and is therefore beyond the scope of the present study.

The observations and the data processing are presented in section 2. To deal with the electric potential, it is necessary to have a circulation model providing the velocity fields whereby the electric model forcing is prescribed. This shallow-water model is presented in section 3, and hereafter, as described in section 4, coupled to an electric-potential model based on Ohm’s law. Subsequently, the datasets are further analyzed and correlations are calculated between the observations and the model results. A measure of the observational range of the cable monitoring system is established in section 5, after which the implications of these results and the possibilities of using the observed potential differences for data assimilation purposes in Baltic circulation models are discussed in section 6.

2. Observations and data handling

From 1 December 1999 to 30 November 2000, the earth’s magnetic fields at the Västervik station and the

potential difference between Visby and Västervik were sampled every 10 s. During this period there were some short episodes of technical difficulties, mainly caused by power cuts, computer failures, and electric pollution from a nearby power cable that was occasionally operated in monopolar mode to test emergency procedures. The occasions when data were missing were few (~ 10) and relatively short ($\sim 1\text{--}30$ h) compared to the length of the entire time series. The gaps were therefore adjusted by replacing the missing measurements with the last recorded signal. The instances of electric pollution were also few and short (~ 20 min) and hence the associated voltage offsets (~ 10 V) were disregarded. An accumulation of errors was noted in the July record, when episodes of power cable electric pollution (confirmed by the operator) took place during a period of severe geomagnetic activity. This ionospherically induced noise was clearly visible in the Planetary Magnetic Three-Hour Indices (viz., the Kp index), and it was decided that periods with a Kp index exceeding 5 were to be excluded from the forthcoming analysis. The potential difference data series consequently includes signals induced by the ocean as well as ionospheric noise, and in order to extract the oceanographic information, it proved necessary to low-pass filter the data. Oceanic tides being almost insignificant in the Baltic (cf. Witting 1911), the filtering procedure will only exclude tides of ionospheric origin. In the present study focus will be on barotropic flows; therefore, it is desirable to reduce the impacts of baroclinicity. This aim was achieved by applying a high-pass filter. The choice of cutoff frequencies was confirmed by calculating the coherence between the locally measured magnetic field and the observed potential difference. For periods longer than 24 h the coherence was low, indicating that the ionospheric influence was negligible, and thus the low-pass cutoff frequency was set to 30 h. Since an earlier study by Pizarro and Shaffer (1998) showed that baroclinic fluctuations mainly manifest themselves on multiweekly time scales, a high-pass filter with a 2-week cutoff was applied to reduce baroclinic effects. A band-pass filter was constructed by combining low- and high-pass Butterworth filters with the cutoff frequencies discussed above. The properties of the raw as well as filtered datasets are summarized in the spectral diagram of Fig. 2. Characteristic features of this diagram are the spikes at the approximate frequencies 0.04, 0.09, and 0.15 cph arising from the ionospheric tides. It is also noteworthy how efficiently these signals are suppressed by the bandpass filtering. (The “hump” located between frequencies of 0.5 and 100 cph is also of ionospheric origin.)

Note, however, that both the higher and lower fre-

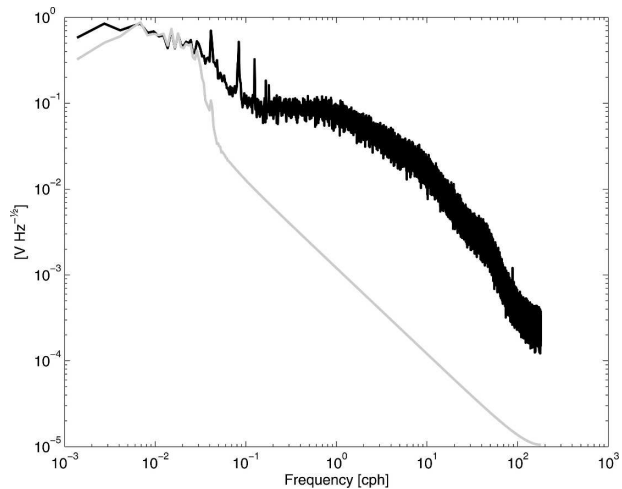


FIG. 2. Spectral analysis diagram for the unprocessed (black) and filtered (gray) potential difference datasets from 1 Dec 1999 to 30 Nov 2000. Filter cutoff frequencies at 30 h and 2 weeks.

quencies of the raw data might contain oceanographic information. This will be further analyzed and investigated in the course of a future study.

3. Modeling the Baltic circulation

An inherent property of motionally induced potential differences is that they are related to the conductivity-weighted average velocity. This quantity bears a degree of resemblance to the barotropic component of the flow, and since we are interested in analyzing the band-filtered potential difference data, a 2D shallow-water model should be appropriate for determining the circulation.

The shallow-water model

The numerical circulation model to be employed was developed by Döös (1999) and is based on the Navier–Stokes equations formulated in spherical coordinates. It has later been used to study seiches in the Baltic, after which the model was augmented to also include bathymetry-dependent friction, yielding successful results (Döös et al. 2004). Most recently it was additionally extended by incorporating tidal forcing, hereby improving the results even further. Technically, the model was implemented by discretizing the governing equations with a horizontal resolution of $1/15^\circ \times 1/30^\circ$ on a C grid using the energy-conserving scheme developed by Sadourny (1975).

1) THE FORCING AND THE MODEL DOMAIN

The forcing was provided by the atmospheric sea surface pressure and the 10-m wind, kindly made available

by the Swedish Meteorological and Hydrological Institute (SMHI) via its operational Mesoscale Analysis system (MESAN). These data were supplied every third hour with a spatial resolution of 0.2° and interpolated linearly to intermediate grid points in both time and space. A wind speed-dependent parameterization of the sea surface stress was employed (Döös et al. 2004). The model domain comprises the semienclosed Baltic Sea, the adjacent Kattegat, and the eastern part of the Skagerrak. The general bathymetry is adopted from Seifert and Kayser (1995), with the modification that for technical-numerical reasons, no depths are allowed to exceed 200 m. Döös et al. (2004) found that this restriction does not exert any significant effects on the larger-scale flow. The western border in the Skagerrak has its end points on the mainlands of Norway and Denmark (cf. Fig. 1). To suppress spurious wave reflection, this longitudinal boundary is treated as a sponge layer (Nycander and Döös 2003). Adjacent to this external boundary, the sea surface elevation was prescribed on the basis of tidal gauge data from Smögen (cf. Fig. 1).

2) THE CIRCULATION MODEL EXPERIMENTS

The model run comprising the period December 1999–November 2000 was initiated from a balanced state (Döös et al. 2004) and carried through with a time step of 20 s to satisfy the Courant–Friedrichs–Lewy criterion. Consonant with the overall focus of the present study, the model output (in the form of velocity and surface height data) was summarized in hourly form. It should furthermore be underlined that the present barotropic model results have been extensively validated on the basis of numerous tidal gauge records from all parts of the Baltic proper, the Gulf of Finland, and the Bay of Bothnia (Döös et al. 2004).

An important constraint when merging the shallow-water and the electric-potential models is that a correct grid transfer be made. That this indeed was the case for the experiments reported here was established by screening the overall results from the shallow-water model run using the continuity equation. It was found that the Skagerrak area must be excluded from the present analysis because of the sponge layer, which, by definition, significantly alters the flow field. In the rest of the modeling domain, the circulation model data can be used to force the electric-potential model, a topic to be considered next.

4. Method for calculating the electric potential

a. Governing equation for the electric potential

Ohm's law relates the electric current density \mathbf{J} to the electric field \mathbf{E} . The former quantity is defined by

$$\mathbf{J} = \sigma(\mathbf{E} + \mathbf{u} \times \mathbf{B}), \quad (1)$$

where σ is the electric conductivity of the medium, \mathbf{u} is the velocity of the charges (here, the ocean current velocity), and \mathbf{B} is the total magnetic field. In the forthcoming analysis, the magnetic field will be regarded as only dependent on the earth's magnetic field \mathbf{F} . Combining the conservation of charge (under the magneto-hydrostatic approximation where $\nabla \cdot \mathbf{J} \approx 0$) with Eq. (1) yields the following equation:

$$-\nabla \cdot (\sigma \mathbf{E}) = \nabla \cdot (\sigma \mathbf{u} \times \mathbf{F}). \quad (2)$$

The electric field can be written as

$$\mathbf{E} = -\nabla \Phi - \partial_t \mathbf{A}, \quad (3)$$

where $\nabla \Phi$ is the electrostatic potential gradient and $\partial_t \mathbf{A}$ is the time derivative of the magnetic vector potential. The present study deals with time scales exceeding that of the diurnal tide, and thus the last rhs term of Eq. (3) is assumed to be negligible (cf. Sanford 1971). This simplification yields a 2D differential equation that can be used to calculate the electric potential by using prescribed main magnetic and velocity fields.

b. Implementing the electric model

Based on a modification of Ohm's law, the electric potential can be determined from the electric field induced by the motion of seawater through the earth's magnetic field. The calculations proceed from a differential equation derived from Eq. (2) integrated through the ocean layer, namely,

$$\nabla \cdot (\Sigma \nabla \Phi) = \nabla \cdot (F_Z \mathbf{T}_\sigma \times \hat{\mathbf{z}}), \quad (4)$$

where Φ is the electric potential and Σ is the depth-integrated seawater conductivity (i.e., the conductance; $\Sigma = \int_H \sigma dz$, where H is the ocean depth). The right-hand side of the equation represents the forcing, dependent on the conductivity transport density $\mathbf{T}_\sigma = \int_H \sigma \mathbf{u} dz$, where σ is prescribed as constant over the entire Baltic domain, \mathbf{u} is the depth-integrated barotropic velocity field originating from the previously described model, and \mathbf{F} is the earth's magnetic field. The velocity field is variable in time and space. The earth's magnetic field, on the other hand, is regarded as only varying spatially since we restrict ourselves to dealing with comparatively short time scales from a geomagnetic perspective. In the electric model the sediments were assumed to be nonconductive. The choice of water and sediment conductivity mainly affects the amplitude of the potential differences. Hence, the electric-model voltage amplitude might exceed that of the observations, as discussed by Sigray et al. (2004) for the region adjacent to the cable. However, the time evolution of

the modeled potential differences is not affected. To avoid spurious electric-field-line deflection in coastal areas, the conductance for grid points with depths below 10 m as well as for terrestrial grid points was prescribed as 10 siemens. This value was decided upon after model experiments had shown that a lower conductance led to the reflection of the electric field lines and a higher conductance yielded unphysical electric currents flowing through solid land.

To facilitate the use of the same grid as in the shallow-water model, Eq. (4) was restated in integral form using Gauss' theorem:

$$\oint_S \nabla \Phi \cdot \hat{\mathbf{n}} dS = \oint_S (F_z \mathbf{T}_\sigma \times \hat{\mathbf{z}}) \cdot \hat{\mathbf{n}} dS, \quad (5)$$

where S is the surface of the grid cell and $\hat{\mathbf{n}}$ is the outward normal. The electric potential is defined at the center of the grid cell, the normal component of the electric field on the bounding surfaces being evaluated by central differences. Translated to the ocean model grid, the electric potential thus is obtained at the Arakawa C-grid “ ξ point,” that is, with the velocities shifted half a cell in each direction. To close this problem, a Dirichlet condition was applied (viz., $\Phi = 0$ on the boundaries). In the electrostatic case herein, this permits electrical charges to move across the boundaries of the model domain, hereby only constraining the solution of the problem to a minimal extent.

c. Model domain size experiments

To avoid spurious electric potential fields arising when solving Eq. (5), the Baltic modeling domain was nested inside a very large stretched grid with terrestrial conductivity but without forcing. The size of the grid cells increased exponentially away from the original model domain. An optimal number of extra grid cells was determined after a series of sensitivity experiments focusing on how the size of an extended grid affects the electric field lines. The model was subjected to test runs for $N = 0, 25, 50$, and 75 extra grid cells in all directions. A Bay-of-Bothnia transect adjacent to Kalix (in close proximity to the modeling domain boundary; cf. Fig. 3) was chosen to study how the calculated potential differences (mirroring the transports) responded to the different nesting conditions. Examining the differences between the resulting voltage time series, $P_{N=0} - P_{N=25}$, $P_{N=25} - P_{N=50}$, $P_{N=50} - P_{N=75}$, their standard deviations were found to be $\sigma = 0.018, 0.0008$, and 0.0003 (V), respectively, for January 2000. This clearly demonstrates that the potential differences converge rapidly as the number of “external” grid cells is increased.

The results from the “50-” and “75-point” experiments are very similar, but since the latter was costly in terms of CPU time, the overall electric field results to be reported here are based on nesting within a 50-point extended grid. As an example of the modeled induced potential fields, the averaged potential field during December 1999–January 2000 is presented in Fig. 3. Here, a striking feature is provided by the concentric patterns in the Baltic proper and in the Bothnian Sea, which are consequences of the gyre circulation observed in the shallow-water model data. It should also be noted that the electric field lines spread smoothly over land and show no signs of being affected by the boundaries, consonant with the expectations underlying the introduction of the stretched external grid and the conductivity assumptions.

d. Nonlocal electric currents

Before exploring the results, the question of the representativity of the measurements should be addressed. An important difference between the water parcels and the electric charges is that the latter spread out over both sea and land, which ultimately might give rise to erroneous transport estimates. For an accurate determination of the properties of the flow, the locally and distantly generated voltages have to be separated. Alternatively, the strength of the latter must be shown to be weak, so as not to seriously influence the measured induced voltage. These distantly generated “nonlocal” electric currents follow horizontal paths, rather than closing in planes containing the vertical axis, as is the case for what could be called the “local” currents. Nonlocal currents can be a dominant effect in cases of flows with strong horizontal divergence (e.g., Tyler and Käse 2001; Tyler 2005), such as tides and other dynamical phenomena mediated by long gravity waves. However, for the lower-frequency circulation we consider, this divergence is much smaller and the nonlocal currents are often negligible [estimates of the relative strength of nonlocal effects for the North Atlantic and for the global ocean circulation can be found in Flosadottir et al. (1997) and Tyler et al. (1997), respectively].

While the model results clearly show that nonlocal currents are present essentially everywhere in and around the Baltic, our primary interest is focused here only on deciding how significant they are in the region close to the cable. To estimate the magnitude of the nonlocal currents in this area, the validity of the assumption $\nabla \cdot \mathbf{J} \approx 0$ was evaluated. This showed that the influence of nonlocal currents in the region adjacent to the cable was negligible, only constituting $\sim 1\%$ of the recorded signal.

Against this background, the modeled potential dif-

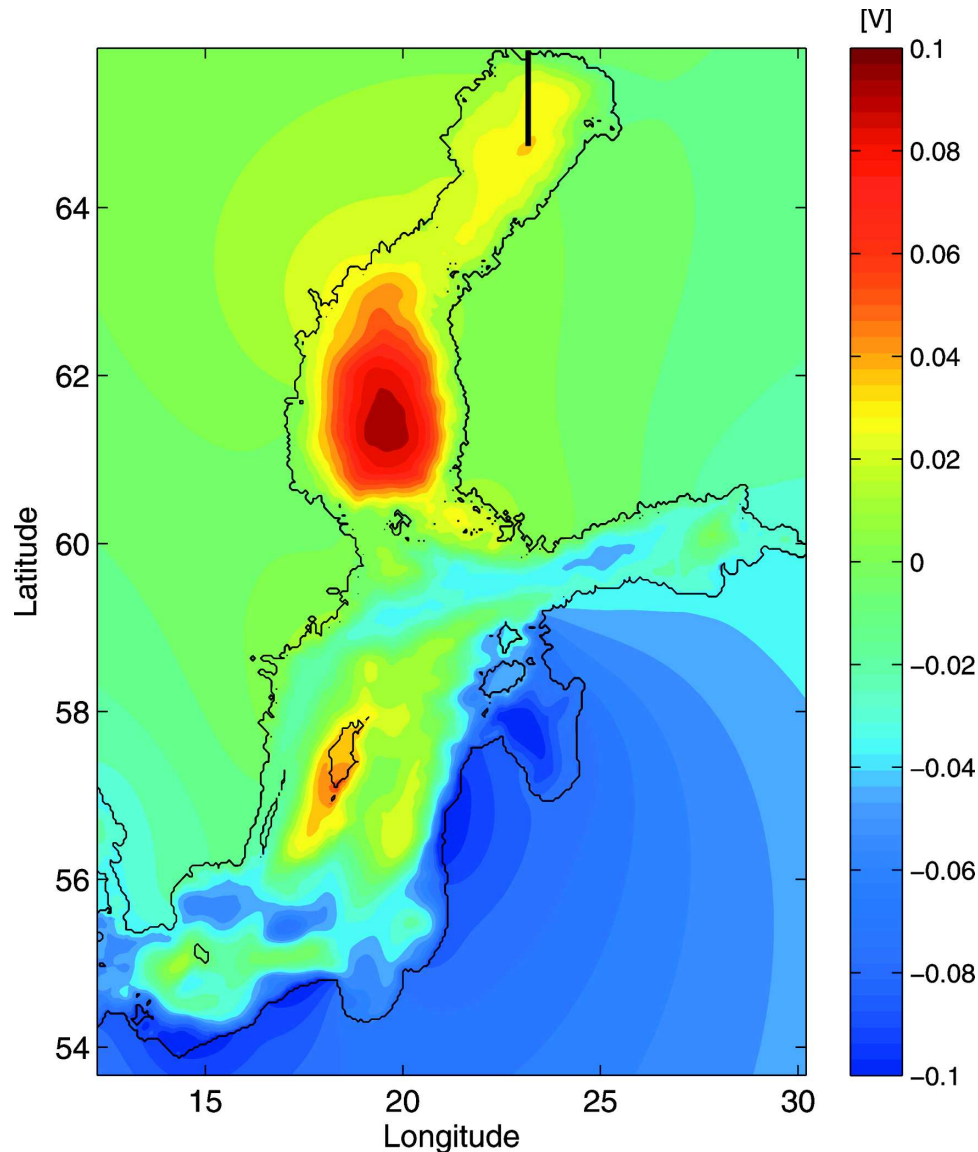


FIG. 3. Example of the average electric-potential field (V) over the Baltic Sea domain during December 1999–January 2000. The Kalix transect in the Bay of Bothnia is shown by the black line.

ferences will next be compared to the in situ observations from the Visby–Västervik transect.

5. Results

As discussed earlier, the modeled barotropic velocities (in which we have a fair degree of confidence; cf. section 2) are used to determine the electric potential fields. Thus, a comparison between these results and the directly measured potential differences should indicate whether the latter contain valid oceanographic information. Since meteorological conditions over the Baltic differ markedly between the seasons, a yearlong

time series from 1 December 1999 to 30 November 2000 was selected for investigation.

a. Local analysis

The observed and modeled data are presented in Fig. 4, where the two time series are somewhat shifted to facilitate visual interpretation. The cable offset cannot be determined exactly (cf. Sigra et al. 2004) and was therefore not specified. (Note that the offset will not affect the forthcoming standard correlation analysis, since this statistical procedure is not sensitive to offsets or amplitudes.) Already a cursory inspection of the figure reveals that the cable and the modeled data covary

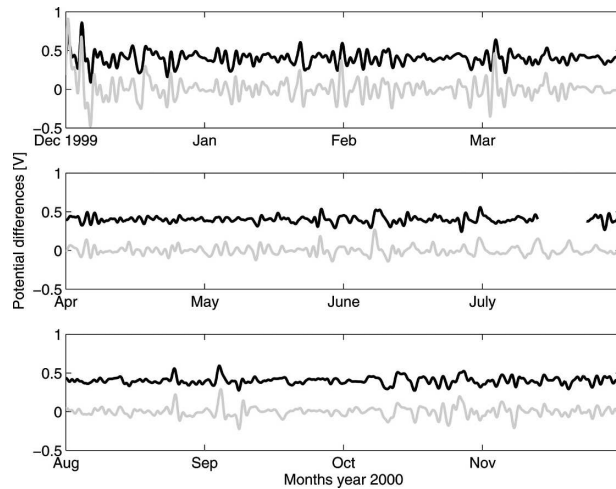


FIG. 4. Comparison between observed (black) and modeled (gray) potential differences (V). The datasets have been shifted slightly for enhanced visibility. (top) December 1999–March 2000, (middle) April–July 2000, and (bottom) August–November 2000.

to a high degree. Because of the seasonality of the atmospheric forcing, the data analysis was focused on two shorter periods, where December 1999–January 2000 was selected as a characteristic winter period and May–June 2000 was taken to represent the summer period (cf. Fig. 5). Since July was a problematic month on purely technical grounds, it was excluded from the analysis. The level of geomagnetic activity, described by the Kp index, was furthermore low for both of these periods, which simplified the analysis. The time series of the selected winter and summer periods are shown in Fig. 5, where the covariability is seen to be reasonably high in both cases. This qualitative judgment is corroborated by the calculated correlations, presented in Table 1. Here the first column demonstrates a close relationship between the modeled transport and voltages, thus showing the internal consistency of the geoelectric model. The results in the second and third column have been included in the table to illuminate the difference between a direct comparison of voltages and an indirect comparison of voltage and transport. The high correlations in the latter case suggest that in the future, observed potential differences can be used for directly estimating transports without the need of invoking electric-potential models.

A pronounced tendency is that the winter period shows overall higher correlations compared to the summer period. The same seasonal variation was noted in the study by Döös et al. (2004). These investigators found that the correlation between the model and the sea level records was lower in summer than during winter. This suggests that the observed potential differ-

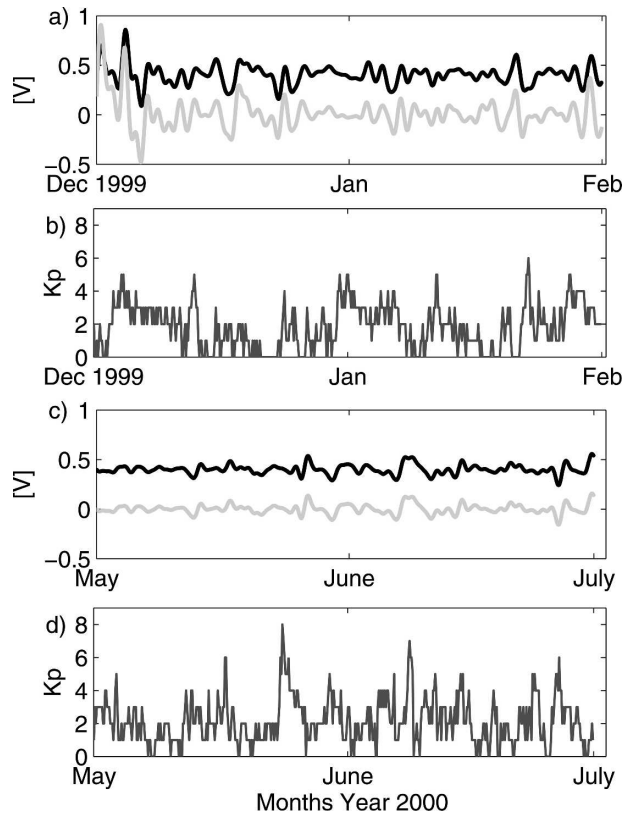


FIG. 5. Comparison between observed (black) and modeled (gray) potential differences (V) for the (a) winter (December 1999–January 2000) and (c) summer (May–June 2000) period. The datasets have been shifted slightly for enhanced visibility. The Kp index is presented for (b) winter and (d) summer. Winter transport conversion factor: 1.9×10^6 ; summer transport conversion factor: 1.4×10^6 .

ences are affected by variations that are not accounted for by the geoelectric model, which in turn is based on shallow-water theory.

It is also noticeable that during winter the correlation between the observed and modeled potential differences is somewhat higher than that between the observed potential difference and the modeled transport. This conforms to expectations, especially during winter when the model performance is best (cf. Döös et al.

TABLE 1. Correlation between bandpass-filtered potential differences (observed as well as modeled) and the modeled meridional transport across the Visby–Västervik transect (with 99.5% significance). Filter cutoff frequencies at 30 h and 2 weeks.

Correlation	Modeled voltage/transport	Observed cable voltage/ modeled voltage	Observed cable voltage/transport
Winter	0.97	0.84	0.77
Summer	0.97	0.73	0.73

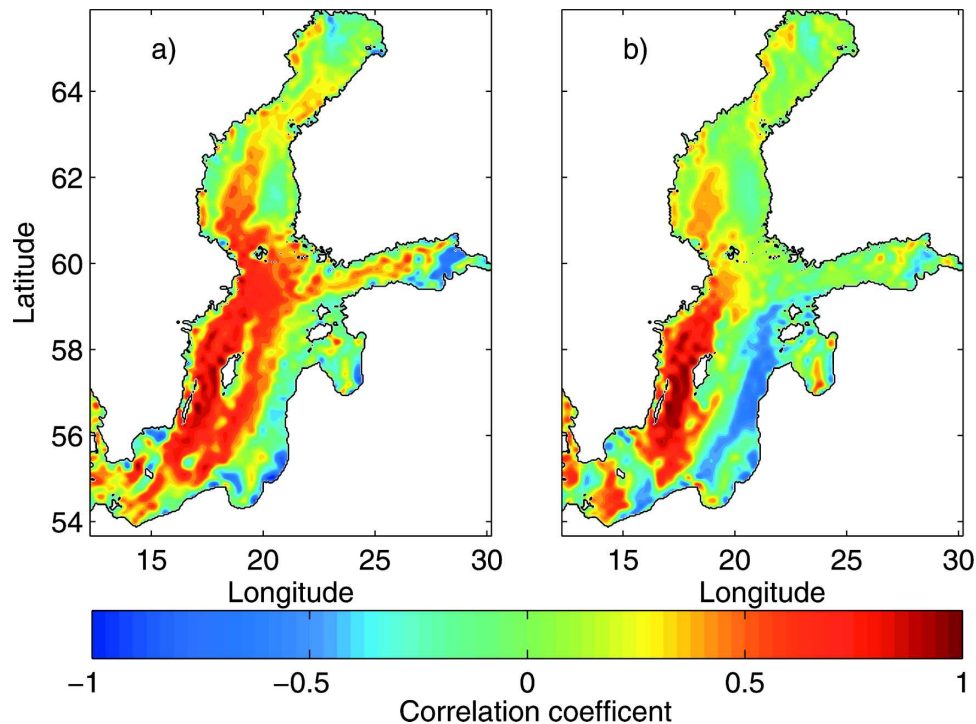


FIG. 6. Correlation between the modeled potential difference and the meridional transports in the Baltic Sea (established with 99.5% significance for essentially the entire area) during the (a) winter and (b) summer period.

2004). It should be kept in mind that the situation is more complex than what first may seem to be the case, since the two statistical estimates have different spatial responses. The correlation between the modeled and observed potential differences is a product of the modeled and the conductivity-weighted average velocities, while the correlation between the observed potential difference and modeled transport is a product of the conductivity-weighted average velocity and the depth-integrated velocity. As a result, the former estimate assigns an even weight to the whole cable transect, whereas the latter has a tendency to overemphasize contributions from the deeper parts of the Visby–Västervik transect. Thus, the weighting in combination with a laterally varying velocity could give rise to the observed difference between the two correlations.

There are strong indications that the cable measurements reflect more of the real flow than do the model results. It is, however, also of interest to determine whether the observed potential differences provide information from other parts of the Baltic, a question to be discussed in what follows.

b. Global analysis

For practical oceanographic purposes, there is frequently an explicit need for new observational methods

that are capable of continuously monitoring conditions over larger spatial scales than those accessible on the basis of point measurements. The cable voltage technique is highly suitable for these kinds of studies. Its integrating property serves to filter out small-scale features, whereas point measurements may be unrepresentative because of local variability. Particularly when planning a monitoring system encompassing the entire Baltic, it is necessary to know the spatial coverage of each measuring device in order to take full advantage of the available resources.

The intent of this larger-scale analysis is thus to provide an estimate of the area over which the cable observations can be regarded as more-or-less representative. Correlations were calculated between the modeled potential differences and the modeled transport in each grid point of the domain. Since the transport across the Visby–Västervik transect is predominantly meridional, the calculated winter and summer correlations as shown in Fig. 6 are based on the modeled transports in the north–south direction. (The correlations with the modeled zonal transports did not contribute any additional information and hence are not presented here.)

As foreshadowed by the discussion in the previous section, correlation maxima are found in the neighborhood of the cable, as clearly seen in Fig. 6. During

winter, high correlations are found over a large part of the Baltic, suggesting broad-scale coherent motion in the Baltic, possibly explained by the more-or-less spatially homogeneous wind stress characterizing this period. During summer, the “highly correlated” area is found in the western part of the Baltic, but a large area with negative correlations is present in the eastern part. This indicates that a basinwide barotropic gyre is present in the Baltic proper during summer, a feature which is highly interesting since the shallow-water model data alone did not suggest its presence. An estimate of the area where the cable-deduced transport estimates can be considered accurate therefore comprises a 100-km-broad zone extending 200 km north and south of the cable.

6. Summary and discussion

In this study, it has been investigated if a cable-based monitoring system can be used for estimating wind-driven barotropic transports across the Visby–Västervik transect in the Baltic Sea. A 1-yr record (1 December 1999–30 November 2000) of potential difference measurements was selected for evaluation of its possible oceanographic content. Since the focus of the investigation is on barotropic flow, the dataset was bandpassed to reduce the influence of baroclinic flow and ionospheric noise. An electric model, adapted to the same physical grid as that used in the well-established shallow-water model (Döös et al. 2004), was developed for the purpose of comparing the observations to a modeled “barotropic” potential difference dataset. The modeling results lived up to expectations and strongly suggest that the cable monitoring system was capable of providing transport data for the Visby–Västervik transect. There are seasonal anomalies in the correlation between the observed and the modeled potential differences, which is explained by the inability of the shallow-water model to fully achieve the summer circulation in the Baltic (Döös et al. 2004), hereby propagating errors to the electric model. It was also observed that the correlation between the modeled and observed potential differences was higher than that between the observed potential differences and the modeled transport. This suggests that the observational dataset is more sensitive to the flow structure across the Visby–Västervik transect than the modeled dataset.

It has furthermore been validated that the monitoring system is capable of estimating the transport over a considerable part of the Baltic, hereby demonstrating the feasibility of using it as an important source of information concerning the Baltic Sea circulation. This global correlation analysis also showed a seasonal dif-

ference in the estimated spatial coverage of the monitoring system. This difference is due to the seasonal variability of the circulation patterns; summer conditions are characterized by a barotropic gyre encompassing the entire Baltic proper, whereas during winter interior broad-scale motion tends to prevail.

To conclude this study, it should be underlined that the results from the correlation analysis indicate that the transports in the well-correlated western part of the Baltic Sea could be used for numerical model assimilation purposes. This could be an important resource for modelers when attempting to improve the existing circulation models, as well as for guiding observers in regards to the siting of new monitoring systems in the Baltic Sea.

Acknowledgments. The authors are very grateful to Dr. Kristofer Döös for providing shallow-water data and for patient support when the modeling was in its primary stage. We also thank Prof. Peter Lundberg for his continuous support in the form of invaluable guidance on the science and the grammar. We would also like to thank Skanova, who made the measurements possible by making their cable available for our purposes. The Miljöfonden managed by the Swedish Association of Graduate Engineers supported part of this work. Valuable support for disseminating the results was given by the Stockholm Marine Research Centre and Stockholm University Donation Grants. Participation by R. H. Tyler was supported by the U.S. Office of Naval Research and the National Aeronautics and Space Administration. We appreciate the valuable comments from the two anonymous reviewers.

REFERENCES

- Döös, K., 1999: Influence of the Rossby waves on the seasonal cycle in the tropical Atlantic. *J. Geophys. Res.*, **104**, 29 591–29 598.
- , J. Nycander, and P. Sigray, 2004: Slope-dependent friction in a barotropic model. *J. Geophys. Res.*, **109**, C01008, doi:10.1029/2002JC001517.
- Flosadottir, A. H., J. C. Larsen, and J. T. Smith, 1997: Motional induction in North Atlantic circulation models. *J. Geophys. Res.*, **102**, 10 353–10 372.
- Larsen, J. C., 1992: Transport and heat flux of the Florida Current at 27°N derived from cross-stream voltages and profiling data: Theory and observations. *Philos. Trans. Roy. Soc. London*, **338**, 169–236.
- Lehmann, A., W. Krauss, and H. H. Hinrichsen, 2002: Effects of remote and local atmospheric forcing on circulation and upwelling in the Baltic Sea. *Tellus*, **54**, 299–316.
- Longuet-Higgins, M. S., M. E. Stern, and H. Stommel, 1954: The electric field induced by ocean currents and movements. *Pap. Phys. Oceanogr. Meteor.*, **8**, 3–27.
- Nycander, J., and K. Döös, 2003: Open boundary conditions for

- barotropic waves. *J. Geophys. Res.*, **108**, 3168, doi:10.1029/2002JC001529.
- Pizarro, O., and G. Shaffer, 1998: Wind-driven, coastal-trapped waves off the island of Gotland, Baltic Sea. *J. Phys. Oceanogr.*, **28**, 2117–2129.
- Sadourny, R., 1975: The dynamics of finite-difference models of the shallow-water equations. *J. Atmos. Sci.*, **32**, 680–689.
- Sanford, T. B., 1971: Motionally induced electric and magnetic fields in the sea. *J. Geophys. Res.*, **76**, 3476–3492.
- , 1982: Temperature transport and motional induction in the Florida Current. *J. Mar. Res.*, **40**, 621–639.
- Seifert, T., and B. Kayser, 1995: A high resolution spherical grid topography of the Baltic Sea. Meereswissenschaftliche Berichte (Marine Science Reports) 9, Institute für Ostseeforschung, Warnemünde, 72–88.
- Sigray, P., P. Lundberg, and K. Döös, 2004: Observations of transport variability in the Baltic Sea by parasitic use of a fiber-optic cable. *J. Atmos. Oceanic Technol.*, **21**, 1112–1120.
- Spain, P., and T. B. Sanford, 1987: Accurately monitoring the Florida Current with motionally induced voltages. *J. Mar. Res.*, **45**, 843–870.
- Tyler, R. H., 2005: A simple formula for estimating the magnetic fields generated by tsunami flow. *Geophys. Res. Lett.*, **32**, L09608, doi:10.1029/2005GL022429.
- , and R. Käse, 2001: A string function for describing the propagation of baroclinic anomalies in the ocean. *J. Phys. Oceanogr.*, **31**, 765–776.
- , L. A. Mysak, and J. M. Oberhuber, 1997: Electromagnetic fields generated by a three dimensional global ocean circulation. *J. Geophys. Res.*, **102**, 5531–5551.
- Witting, R., 1911: Tides in the Baltic Sea and the Gulf of Finland (in Swedish). *Fennia*, **29**, 1–84.